

Nuclear-Structure Effects in High-Energy (p,n) Reactions

JACQUES B. J. READ* AND J. M. MILLER

Columbia University, New York, New York

(Received 28 June 1965)

The cross sections for the (p,n) reaction at 370 MeV with Ca^{44} , Ca^{48} , V^{51} , Cr^{54} , and Ag^{109} have been measured to be 2.0 ± 0.2 , 2.3 ± 0.3 , 2.2 ± 0.2 , 0.72 ± 0.15 , and 1.45 ± 0.15 mb, respectively. These results, along with others in the literature, are analyzed in terms of a semiclassical model that considers the direct ejection of the least-bound and the next-least-bound neutrons from the target nucleus by a quasielastic scattering of the incident proton. The spatial distribution of the struck neutrons is taken as that given by the appropriate harmonic-oscillator wave functions. Estimates of the binding energies of neutrons in the first level below that which is least bound result from this analysis.

I. INTRODUCTION

SPALLATION reactions induced by high-energy protons have long been regarded as occurring through a two-step process. The first step is a cascade of one or more high-energy nucleon-nucleon collisions, which is completed within the first 10^{-22} sec of the reaction. This is followed by the second step, the much slower decay of the residual excited nucleus that has been formed. Reasonable agreement between calculated final-product distributions and observed formation cross sections has been reported using Monte Carlo computer simulation of the cascade step and evaporation calculations for the subsequent emissive decay. It is, unfortunately, difficult to take shell effects into account in a simulative calculation without introducing somewhat artificial parameters, and the Monte Carlo method is thus best suited to the treatment of the more complex reactions in which there are many intranuclear collisions and shell effects tend to be averaged out. Certain of the simpler spallation reactions, however, are tractable by nonsimulative calculations, namely, those involving a "cascade" step consisting of only a single high-energy nucleon-nucleon collision. If the residual nucleus received insufficient excitation energy to emit a particle, then the reaction is even more easily treated.¹⁻³ In the region of bombardment energies in which elastic nucleon-nucleon collisions predominate, these simple spallations are the (p,n), ($p,2p$), and (p,pn) reactions. Although cascades involving more than one high-energy collision could conceivably contribute to the yield of these reaction products, it can easily be seen that such contributions must be very small.

At bombardment energies below about 400 MeV, the (p,n) reaction can occur through only one of the many possible combinations of the two spallation steps: the incident proton must collide with and eject a loosely bound target neutron in such a manner that the sum of the particle excitation energy of the proton after the

collision (U) and the hole excitation energy left by the removal of the neutron (E) must be insufficient to permit the emission of a particle from the residual nucleus (see Fig. 1). The high-energy neutron created in this collision must of course leave the target nucleus without participating in another collision that would increase the excitation energy to the point where another particle would be emitted. Above 400 MeV, inelastic proton-neutron collisions become more and more likely, and complicate the situation by adding meson-producing reactions which can yield the same product nucleus as the (p,n) reaction.

Two important properties of the (p,n) reaction are obvious: (1) neutrons within the diffuse edge of the target nucleus are favored as collision partners of the incident proton, since their location permits the energetic neutron created in the collision a much better chance to escape the nucleus without imparting further excitation energy; and (2) neutrons which are loosely bound to the target nucleus are also favored, since their extraction will leave less hole excitation energy in the residual nucleus. These two effects compound each other, in the sense that nucleons which have comparatively large expectation values for their radii are, in general, comparatively loosely bound to the nucleus. Due to the importance of these two properties to this reaction, the relative magnitude of (p,n) cross sections should be expected to be predictable in terms of the binding energies of single-particle neutron states of the

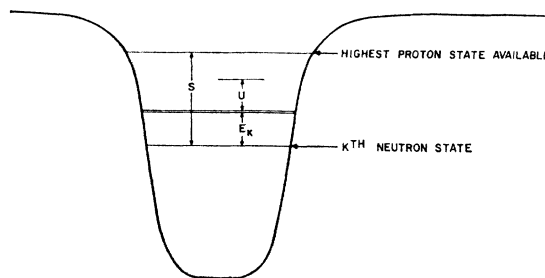


FIG. 1. Diagram illustrating the division of the total excitation energy of the residual nucleus into two parts: the proton excitation energy U and the neutron hole excitation E_k . Their sum must be less than S [defined in Eq. (4)] in order to yield the (p,n) product upon de-excitation.

*Present address: Lawrence Radiation Laboratory, Livermore, California.

¹ P. A. Benioff, Phys. Rev. **119**, 324 (1960).

² N. T. Porile and S. Tanaka, Phys. Rev. **130**, 1541 (1963).

³ P. L. Reeder and S. S. Markowitz, Phys. Rev. **133**, B639 (1964).

shell model and their spatial distributions within the nucleus. It is our purpose here to investigate this relationship.

Of the three simplest spallation reactions listed above, the most thoroughly investigated to date has been the high-energy (p, pn) reaction.^{1,2,4,5} Cross sections for this reaction are typically two to three times larger than those of the $(p, 2p)$ reaction, and one or two orders of magnitude larger than those of the (p, n) reaction. In the region of target mass numbers between fifty and eighty, the (p, pn) cross section has been found to vary abruptly with the target's neutron number. By means of Benioff's calculations,¹ this variation has been interpreted as an indication that, after a certain neutron number has been exceeded, buried subshells have become sufficiently tightly bound that the hole excitation energy occasioned by their removal is larger than the neutron separation energy of the residual nucleus.² Since a subshell must be either available for the (p, pn) reaction or unavailable, the (p, pn) cross section is not very sensitive to fluctuations in single-particle neutron energies with neutron number. The degree to which a target-neutron state contributes to the (p, n) reaction, however, depends upon the allowed range of energies of the low-energy proton created in the initial charge-exchange collision, and not just upon whether or not the neutron is sufficiently loosely bound. As a result (p, n) cross sections vary erratically with target neutron number, whereas (p, pn) cross sections tend to be approximately the same over regions of neutron number.

In the work described here, several (p, n) cross sections in the regions of the closed neutron shells at $N=28$ and the closed proton shells at $Z=20$ and $Z=28$ were compared to calculations analogous to Benioff's. As with Benioff's model,¹ isotropic harmonic-oscillator eigenfunctions have been employed to approximate the nucleon density distribution in the diffuse edge of the target nucleus, and zero-angle scattering and the applicability of free-particle nucleon-nucleon cross sections have been assumed.

II. EXPERIMENTAL

Bombardments of calcium, vanadium, chromium, and silver were made using the internal beam of the Nevis synchrocyclotron. Vanadium and silver were bombarded as metal foils, 1 and 5 mils thick, respectively; chromium was irradiated as metallic powder, 300 mesh and finer; and calcium was irradiated as CaF_2 and CaCO_3 powders. The proton intensity in the foil targets was measured by placing $\frac{1}{2}$ -mil high-purity aluminum monitor foils on both sides of the target foil. The powder targets were monitored by mixing fine aluminum powder (500 mesh and finer) uniformly with

the target material. The mixing was done using several grams of each of the two powders, and milligram quantities of these mixtures were taken for each target. An internal monitor was employed in the bombardments of separated calcium isotopes, where insufficient material was available for adequate insurance of uniformity of mixing.

For irradiation, the powder target material was placed in a depression stamped in 1-mil aluminum foil, and the foil folded over to seal in the powder and compress it. The depression was 25 mm by 2 mm for the natural isotopic abundance targets, and 15 mm by 1 mm for the enriched isotopes. The targets were bombarded with the largest dimension of the aluminum envelope forming the leading edge of the target assembly. Cross sections for the $\text{Al}^{27}(p, 3pn)\text{Na}^{24}$ reaction used in monitoring the beam were taken from the compilation by Bruninx.⁶

Chemical separations were performed by standard methods.⁷ Chromium was separated by the extraction of perchromic acid into ethyl acetate, and was counted as either BaCrC_4 , Ag_2CrO_4 , or Cr_2O_3 . Cadmium was separated by precipitation of CdS after repeated AgCl scavengings and counted as the sulfide. Calcium was repeatedly reprecipitated as alternately CaCO_3 and CaC_2O_4 , and finally counted as the carbonate. Potassium was separated by repeated reprecipitation of KClO_4 , and was counted as both the perchlorate and chloroplatinate to insure the absence of ammonium and sodium salts. Sodium was precipitated as hydrous zinc uranyl acetate and counted in this form. In early bombardments, sodium was also counted as the perchlorate as well as the zinc uranyl acetate in order to confirm the gravimetric factor for the latter. To assure complete washing of the precipitate in the sodium separation, 30 mg of sodium carrier were used, and the zinc uranyl acetate precipitate was washed with small amounts of water and ethanol. Although a large fraction of the precipitate was redissolved with this treatment, there was a sufficient amount left after washing owing to the large amount of carrier which had been added. This procedure was found necessary to remove excess heavy metal salts from the precipitate. Scandium was repeatedly reprecipitated as the hydroxide, and the final precipitate was transferred into a small crucible and fired to convert it into Sc_2O_3 , which was then counted.

The Na^{24} contained in the aluminum monitor foils was determined by counting coincidences between the 1.37-MeV gamma and beta rays. Standards having known disintegration rates at various gamma energies were purchased from the National Bureau of Standards, borrowed from the Chemistry Department of Brookhaven National Laboratory, or made and calibrated in

⁶ E. Bruninx, CERN Report No. 61-1, Geneva, 1961 (unpublished).

⁷ *Subcommittee on Radiochemistry Monographs* (National Academy of Sciences-National Research Council, Washington, D. C., 1961).

⁴ L. P. Remsberg and J. M. Miller, *Phys. Rev.* **130**, 2069 (1963).

⁵ J. R. Grover and A. A. Caretto, *Ann. Rev. Nucl. Sci.* **14**, 51 (1964).

this laboratory by coincidence techniques. By their use, peak efficiencies of a 3-in.-by-3-in. NaI crystal scintillator at these energies were measured with an accuracy believed to be about 1%. All counting was done using this crystal at as low a geometry as practical and with pulse-height analysis. With the exceptions of Cd¹⁰⁹, Sc⁴⁶, and some samples containing Sc^{44g}, all samples were counted over at least three half-lives. The Cd¹⁰⁹ was determined by counting the decay of the 39-sec Ag¹⁰⁹ daughter, using the internal conversion data of Wapstra and Van der Eijk,⁸ which indicates 95.0% conversion of the 0.0877-MeV Ag¹⁰⁹ radiation.

Since the simpler spallation reactions, by their very nature, impart comparatively little momentum to the residual nuclei produced, loss of activity from the targets by recoil is negligible for targets having area densities greater than about 1 mg per cm². A problem that can easily become serious, however, is the production of (p, n) product nuclei in the target by the reaction of secondary protons, as formation cross sections for these products are typically as much as two or three orders of magnitude larger at incident proton energies of several MeV than they are for 370-MeV protons. From data on the average number of low-energy protons produced in each inelastic collision⁹ and from the exhaustive study by Koch¹⁰ of the effects of secondary protons on the Ni⁶⁴(p, n)Cu⁶⁴ reaction, we concluded that secondaries can be considered to have a negligible contribution to the powder target cross sections measured here, and to contribute less than 10% of the observed V⁵¹(p, n)Cr⁵¹ cross section. Although it is more difficult to estimate an upper limit to the secondary contribution to the silver cross sections, it is believed to be less than 20% of the measured cross sections. Because of the long half-life of the product in this reaction, it was not feasible to use thinner silver targets.

Cross sections for the reactions Ca⁴⁸($p, pn + 2p$)Ca⁴⁷, Ca⁴⁸($p, 2n$)Sc⁴⁷, and Ca⁴⁸(p, n)Sc⁴⁸ have been reported by Levenberg *et al.*¹¹ from measurements using extremely large targets of natural isotopic abundance calcium carbonate. These cross sections are roughly 30, 50, and 100% greater, respectively, than those found in this work, and it is apparent that much of the lack of agreement is caused by secondary contributions.

Other sources of experimental error in the powder targets include: (1) the recoil into the powder of Na²⁴ which was made in the aluminum envelope; (2) the production of Na²⁴ in the powder by spallation of the calcium or chromium in addition to the spallation of the aluminum; and (3) in the case of the calcium targets, the interference of other reactions involving the other calcium isotopes also present. The first two errors listed

above can be greatly minimized by keeping the aluminum concentration in the powder sufficiently high that these two extraneous methods of introducing Na²⁴ into the powder can account for only a small fraction of the total Na²⁴ found. To make certain that these sources of error were properly estimated, a series of three bombardments of different thicknesses of pure calcium carbonate of natural isotopic abundance was carried out at 370 MeV, and the ratios of Na²⁴ to both Ca⁴⁷ and K⁴³ were measured for each target. Since the area each of these targets presented to the incident beam was kept constant regardless of its thickness, the number of Na²⁴ recoils into the powder from the aluminum envelopes should be proportional to the number of protons passing through each target. The numbers of protons passing through each target is in turn measured by the ratios of the number of either Ca⁴⁷ or K⁴³ nuclei produced in the target to the target thickness. It was thus possible to estimate the contributions to the total Na²⁴ production from the first two sources of error listed above by empirically fitting curves of the Na²⁴/Ca⁴⁷ and Na²⁴/K⁴³ ratios plotted against the reciprocal of the target thickness. An estimated upper limit to the Ca⁴⁰($p, 9p6n$)Na²⁴ cross section was found to be 480 μ b. Since the V⁵¹($p, 12p16n$)Na²⁴ cross section in this energy region has been found by Rudstam¹² to be 20 to 30 μ b, the chromium spallation cross section for forming Na²⁴ was assumed to be negligibly small. Using the rough estimation of these errors obtained from these three bombardments, corrections of about 5% to nearly 15% were subtracted from the amounts of Na²⁴ found in the other powder target bombardments.

The net cross section for the production of Ca⁴⁷ from Ca⁴⁸ both directly from the (p, pn) reaction and by decay after the ($p, 2p$) reaction was conveniently large, 71.3 \pm 5.4 mb at 370 MeV, and had the advantage that its product, Ca⁴⁷, could be made by no other competing reaction. For these reasons it was chosen as an internal monitor for the series of enriched-calcium bombardments. The error given for this cross section is the standard deviation of the mean for four independent measurements, and its value is given relative to the Al²⁷($p, 3pn$)Na²⁴ cross section, taking the latter to be 11.2 mb at 370 MeV.⁸

Two enriched-isotope samples of calcium were purchased from the Oak Ridge National Laboratory, one containing 9.56% Ca⁴⁴ and 39.7% Ca⁴⁸, and the other 98.6% Ca⁴⁴ and 0.01% Ca⁴⁸, so that with natural calcium, three different mixtures of these two isotopes were available for bombardment. Neither of the enriched samples nor natural calcium contains enough Ca⁴⁶ to permit easy measurement of simple spallation cross sections for this nuclide, and the second enrichment mentioned above is virtually without it (less than 20 ppm). The isotopic abundances claimed by the

⁸ A. H. Wapstra and W. Van der Eijk, Nucl. Phys. 4, 325 (1957); 4, 695 (1957).

⁹ G. Bernardini, E. T. Booth, and S. J. Lindenbaum, Phys. Rev. 85, 826 (1952).

¹⁰ R. C. Koch, thesis, University of Chicago, 1955, (unpublished)

¹¹ I. Levenberg, V. Pokrovsky, and I. Yutlandov, Nucl. Phys. 41, 504 (1963).

¹² G. Rudstam, thesis, University of Uppsala, Sweden, 1956, (unpublished).

TABLE I. Calcium spallation cross sections (in millibarns) at 370 MeV.

$\text{Ca}^{48}(p, p\pi+2p)\text{Ca}^{47}$	71.3 ± 5.4	
$\text{Ca}^{48}(p, n)\text{Sc}^{48}$	2.30 ± 0.25	
$\text{Ca}^{48}(p, 2n)\text{Sc}^{47}$	5.50 ± 0.43	
$\text{Ca}^{48}(p, 3n)\text{Sc}^{46}$	5.56 ± 0.50	
$\text{Ca}^{48}(p, 5n)\text{Sc}^{44(m+\sigma)}$	2.0 ± 0.2	$[m/g=0.47 \pm 0.10]$
$\text{Ca}^{48}(p, 2p4n)\text{K}^{43}$	27.0 ± 4.0	
$\text{Ca}^{48}(p, 2p5n)\text{K}^{42}$	16.0 ± 2.0	
$\text{Ca}^{44}(p, n)\text{Sc}^{44(m+\sigma)}$	2.0 ± 0.2	$[m/g=0.21 \pm 0.03]$
$\text{Ca}^{44}(p, 2p)\text{K}^{43}$	14.0 ± 2.0	
$\text{Ca}^{44}(p, 2p\pi)\text{K}^{42}$	28.0 ± 3.0	

supplier were assumed to be true, and the claimed precisions of their analyses were interpreted as the standard deviations of the abundances. For the natural isotopic abundances, the values given by the Nuclear Data Sheets¹³ were taken, with the standard deviation assumed to be ± 2 in the least significant figure reported.

In each calcium bombardment, K^{42} , K^{43} , Ca^{47} , Sc^{44m} , $\text{Sc}^{44\sigma}$, Sc^{46} , Sc^{47} , and Sc^{48} were sought as products, although some of these could not be found in measurable amounts in one or another of the enrichments used. Sc^{43} was detected in most scandium fractions, but could not be adequately determined in the presence of the $\text{Sc}^{44\sigma}$.

The data were analyzed by the IBM 7094 at the Columbia Computer Center. The program first calculated the most probable ratios of the numbers of product nuclei formed for each pair of products at each enrichment, and then solved the series of simultaneous equations relating these ratios to the individual reaction cross sections and isotopic composition of target, while concurrently calculating the propagation of errors. The most probable values of the measured cross sections for calcium targets are listed in Table I, along with their standard deviations. Also included in Table I are the observed metastable-to-ground-state production ratios for Sc^{44} . Calculations were made both including and excluding Ca^{46} as a contributor to the product distribution. The results of these two calculations were within estimated errors, except for the $\text{Ca}^{44}(p, 2p)\text{K}^{43}$ reaction, whose cross section was artificially increased by an obviously nonphysical enormous negative $\text{Ca}^{46}(p, 2p2n)\text{K}^{43}$ cross section. In all cases, the estimated errors were increased by including Ca^{46} , and the Ca^{46} cross sections that were calculated had no statistical significance. The values reported in Table I are those calculated by ignoring the presence of Ca^{46} , since it appeared likely that the small amounts of this nuclide present in the targets had no detectable effect upon the amounts of products of interest.

The (p, n) cross sections measured in this work, along with others in this energy region, are collected in Table II. The $\text{Ag}^{109}(p, n)\text{Cd}^{109}$ cross section was measured at four energies, all of which are reported in Table II. An

¹³ *Nuclear Data Sheets*, edited by K. Way *et al.* (National Academy of Sciences-National Research Council, Washington, D. C., 1960).

old value of this last cross section by Kofstad,¹⁴ 3.4 mb at 340 MeV, antedates by a few years the first reliable investigation of the decay scheme of the Cd^{109} product and was determined by counting Cd^{109} x rays with a Geiger tube, with an underestimation by about a factor of two of the number of x rays per disintegration. Kofstad used 10-mil silver foil targets, and if all other factors were correctly estimated, his value for this cross section would have been 1.7 mb. If 20% of this cross section was due to additional secondary contribution, this value would be in agreement with that obtained in the present work, where we have used targets half as thick as Kofstad's.

The $\text{Cu}^{65}(p, n)\text{Zn}^{65}$ cross section reported by Batzel *et al.*¹⁵ was measured in a target sufficiently thin to avoid excessive secondaries; however, the Zn^{65} was determined by counting gamma rays through an aluminum absorber with a gas-filled proportional counter, the gamma efficiency of which was only approximately known. An accuracy of 50% was assumed in treating this last cross section.

III. DISCUSSION

If the (p, n) reaction is assumed to proceed through a collision between the incident proton and a target neutron in a single-particle state, then, under the assumption that the target nucleons are independent, a fraction of the total (p, n) cross section may be associated with each neutron state k available to the reaction

$$\sigma(p, n) = \sum_k \sigma_k' \quad (1)$$

We may write an expression for the contribution of the k th neutron state to the total (p, n) cross section by using the impulse approximation and the approximation that the trajectories of the incoming proton and outgoing neutron are colinear. Since the orientation of the target nuclei with respect to the beam is random, we have made the further assumption that the target may

TABLE II. Collected (p, n) cross sections.

Target	Energy (MeV)	$\sigma(p, n)$ (mb)	Reference
Ca^{44}	370	2.0 ± 0.2	This work
Ca^{48}	370	2.30 ± 0.25	This work
V^{51}	370	2.2 ± 0.2	This work
Cr^{52}	370	1.45 ± 0.10	Ref. 4
Cr^{54}	370	0.72 ± 0.15	This work
Fe^{56}	370	0.92 ± 0.06	Ref. 4
Ni^{64}	416	0.97 ± 0.11	Ref. 10
Cu^{65}	340	0.74 ± 0.37	Ref. 15
Ag^{109}	380	1.45 ± 0.15	This work
Ag^{109}	290	1.70 ± 0.15	This work
Ag^{109}	210	3.00 ± 0.15	This work
Ag^{109}	140	3.22 ± 0.15	This work

¹⁴ P. K. Kofstad, Lawrence Radiation Laboratory, Berkeley, California, Report No. UCRL 2265, 1953 (unpublished).

¹⁵ R. E. Batzel, D. R. Miller, and G. T. Seaborg, Phys. Rev. 84, 671 (1951).

be treated as a sphere of radius R .

$$\sigma_k' = 2\pi \int_{\Omega_k} \frac{d\sigma}{d\Omega} \int_0^R b db \int_0^{2(R^2-b^2)^{1/2}} \rho(b, z') dz' \times \exp\left[-\sigma_p \int_0^z \rho(b, z') dz'\right] \times \exp\left[-\sigma_n \int_z^{2(R^2-b^2)^{1/2}} \rho(b, z') dz'\right] \rho_k(z, b) dz, \quad (2)$$

where b = impact parameter between proton and target nucleus, z = distance traveled by proton in the nucleus before collision with the k th neutron, z' = variable of integration along z axis, σ_p = average proton-nucleon cross section, σ_n = average neutron-nucleon cross section, $\rho(b, z')$ = density of target nucleus at the point (b, z') , $\rho_k(b, z')$ = density of the k th neutron state at the point (b, z') , R = maximum allowed impact parameter, $\partial\sigma/\partial\Omega$ = differential p - n scattering cross section, and Ω_k = solid p - n scattering-angle allowed to the k th neutron state (to be discussed later in the text).

In Eq. (2) the two exponential factors estimate, respectively, the probability that a proton will penetrate to the collision site at z without previous interaction, and the probability that the neutron will escape from the nucleus without further interaction. The approximation has been made that the nucleon density experienced by the incoming proton and outgoing neutron are identical. In Benioff's analogous treatment of the $(p, pn\pi)$ reactions¹ at much higher energies, the nucleon density penetrated by the outgoing particles was obtained by removing the density of the struck neutron from the total density of the original target. For a better estimation of the (p, n) cross section than we have attempted here, however, we would not only have to remove the density of the struck neutron but also to make an allowance for the additional proton now contributing to the potential well. Hopefully, the two deleted effects will tend to cancel each other, and it was felt that any error incurred by using this approximation would be negligible compared to that incurred by employing approximate eigenfunctions in the estimation of the densities themselves. The refraction of the proton and neutron by the potential-energy gradients in the nucleus has been ignored also.

The compilation by Hess¹⁶ of free-particle scattering data contains graphs of the total elastic n - p and p - p scattering cross sections as a function of energy. From this compilation on nucleon-nucleon scattering data, σ_p and σ_n were both set equal to 30 mb in the evaluation of Eq. (2). The total nucleon and k th neutron state densities were replaced by the squares of the suitably normalized (normalized to the occupation number of each state) isotropic harmonic-oscillator radial eigenfunctions. In this use of oscillator eigenfunctions,

¹⁶ W. N. Hess, Rev. Mod. Phys. **30**, 368 (1958).

TABLE III. Coefficients a_k for those neutron states possibly contributing to the (p, n) reaction [see Eq. (8)].

Target	State, k	Trial values of oscillator frequency as $\hbar\omega$ in MeV.			
		7	8	9	10
Ca ⁴⁴	$1f_{7/2}$	1.53	1.39	1.26	1.16
	$1d_{3/2}$	1.19	1.04	0.93	0.82
Ca ⁴⁸	$1f_{7/2}$	2.87	2.56	2.33	2.13
	$1d_{3/2}$	1.07	0.96	0.83	0.73
V ⁵¹	$1f_{7/2}$	2.69	2.39	2.16	1.91
	$1d_{3/2}$	1.02	0.88	0.76	0.66
Cr ⁵²	$1f_{7/2}$	2.67	2.37	2.12	1.93
	$1d_{3/2}$	1.00	0.86	0.74	0.65
Cr ⁵⁴	$2p_{3/2}$	0.68	0.62	0.57	0.53
	$1f_{7/2}$	2.57	2.26	2.01	1.80
Fe ⁵⁶	$1d_{3/2}$	0.96	0.82	0.71	0.62
	$2p_{3/2}$	0.66	0.60	0.55	0.51
Ni ⁶⁴	$1f_{7/2}$	2.48	2.19	1.93	1.74
	$1d_{3/2}$	0.92	0.79	0.68	0.59
Cu ⁶⁵	$1f_{5/2}$	1.08	0.95	0.84	0.74
	$2p_{3/2}$	1.20	1.08	0.98	0.90
Ag ¹⁰⁹	$1f_{7/2}$	2.15	1.89	1.67	1.48
	$1f_{5/2}$	1.06	0.93	0.82	0.73
Ag ¹⁰⁹	$2p_{3/2}$	1.17	1.05	0.96	0.88
	$1f_{7/2}$	2.12	1.86	1.64	1.46
	$2d_{3/2}$	1.07	0.95	0.86	0.79
	$1g_{7/2}$	1.48	1.28	1.13	1.00
	$1g_{9/2}$	1.85	1.62	1.42	1.25
	$2p_{1/2}$	0.30	0.27	0.24	0.22

single-particle levels with the same principle and azimuthal quantum numbers but differing spins have identical spatial distributions.

To insure that collisions in the diffuse edge were not underestimated by prematurely cutting off high-impact-parameter collisions, the maximum impact parameter considered R was set equal to 10 F. This wasted some computer time, since the (p, n) reaction-probability was negligible at these extreme impact parameters, but the safeguard was convenient in coding the program. Integration over the variables b , z' , and z was performed by area sums using the Columbia Computer Center's IBM 7094. The intervals over which areas were summed were never allowed to exceed 0.1 F, and in nearly all of the summations the intervals were very much smaller. Errors in numerical integration were estimated at less than 1%. Output was given in the form of tables of dimensionless coefficients a_k such that Eq. (1) could be expressed in the following form:

$$\sigma(p, n) = \sum a_k \int_{\Omega_k} \frac{\partial\sigma}{\partial\Omega} d\Omega. \quad (3)$$

These coefficients are somewhat analogous to Benioff's "fractional availabilities."¹¹ Table III contains the calculated values of a_k for the uppermost neutron states of the target nuclei considered here for various choices of the value of the oscillator frequency.

To perform the required integration over solid angle and the subsequent summation in Eq. (3), we must first decide which neutron states are sufficiently loosely bound to contribute to the reaction and then estimate

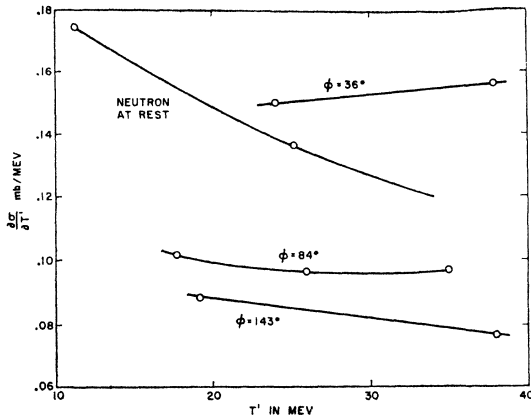


FIG. 2. Differential (p - n) elastic-scattering cross section with respect to the resultant proton kinetic energy in the laboratory system T' . Calculation has been made assuming the initial laboratory energy of the proton was 395 MeV, and the initial laboratory energy of the neutron was 25 MeV; ϕ is the laboratory angle between the initial momenta of the two particles. The case in which the neutron was initially at rest has been included for comparison. The claimed precision of the $\partial\sigma/\partial\Omega$ data from which these points were obtained averages 10%. The lines through the experimental points are for convenience in reading the graph only. Since when $\phi = 180^\circ$, $\partial\sigma/\partial T' = 0$ at $T' = 25$ MeV, the curve at 143° must have a more pronounced minimum at 25 MeV than that at 84° .

the solid angle of scattering over which the net excitation energy given the residual nucleus will be insufficient for particle evaporation. If the possibility of gamma competition in the decay of the residual nucleus and the so-called "rearrangement energy" are ignored, then the simplest criterion for the (p , n) reaction is to assume that the sum of the single-particle proton excitation energy U and the hole excitation energy obtained by removing a k neutron to form the residual nucleus E_k is less than the separation energy S of the least bound nucleon in the residual nucleus.

$$S \geq E_k + U \quad (4)$$

Using this inequality as a criterion is equivalent to assuming that the potential energies of the neutron and proton are unchanged by the collision. Note also that no restriction upon the kinetic energy of the proton after the collision other than that in the inequality above has been made, i.e., the state into which the proton is captured to form the residual nucleus is not considered.

We must now integrate the differential p - n elastic-scattering cross section over the solid angle which includes all collisions in which the laboratory system kinetic energy of the proton after the collision is between the kinetic energy of the least bound proton in the residual nucleus (i.e., $U=0$) and $S-E_k$ more than this energy (i.e., $U=S-E_k$). Collisions after which the kinetic energy of the proton is less than that of the least bound proton in the residual nucleus are, of course, forbidden by the Pauli exclusion principle. If the target neutrons were stationary within the target nucleus, then the

integration required in Eq. (3) could be performed simply by graphically integrating $2\pi \sin\theta(\partial\sigma/\partial\Omega)$ over the allowed range of center-of-mass scattering angle, using experimental tables of n - p elastic-scattering differential cross sections. The momentum distribution of neutrons in the target nucleus cannot be ignored, however, since it has the effect of considerably altering the solid angle available to the reaction. Further, consider, as an example, the collision with a neutron of 25-MeV kinetic energy within the target nucleus. We may examine two extreme instances of scattering between the incident proton and this bound neutron, namely, the instance in which the momenta of the proton and neutron are in the same direction, and the instance in which they are in opposite directions. In the first case, the relative velocity between the two particles is such that we must use $\partial\sigma/\partial\Omega$ data for the n - p elastic scattering at 225 MeV in performing the integration in Eq. (3), and in the second case we must use $\partial\sigma/\partial\Omega$ data at 620 MeV.

If we write T and T' for the kinetic energies of the proton in the laboratory system before and after the collision, respectively, T_n for the kinetic energy of the bound neutron, ϕ for the angle between the momenta of the two particles in the laboratory system, and θ for the center-of-mass scattering angle of the proton, we can derive the transformation of $\partial\sigma/\partial\Omega$ into $\partial\sigma/\partial T'$.

$$\frac{d\sigma}{dT'} = \frac{d\sigma(\theta, \phi)}{d\Omega} \times \frac{2\pi \{2/[\frac{1}{2}(T_n + T) - (\cos\phi)(TT_n)^{1/2}]\}^{1/2}}{T_n^{1/2} \sin\phi \cos\theta - (T^{1/2} + T_n^{1/2} \cos\theta)\sin\theta}, \quad (5)$$

where

$$T' = \frac{1}{2}(T_n + T) + \left[\frac{1}{4}(T + T_n) - \frac{1}{2}T^{1/2}T_n^{1/2} \cos\phi\right]^{1/2} \times [T^{1/2} \cos\theta + T_n^{1/2}(\cos\phi \cos\theta + \sin\phi \sin\theta)]. \quad (6)$$

The differential scattering cross section has been written as a function of θ and ϕ as a reminder that n - p scattering data at varying bombardment energies must be used when considering various ϕ values. When these last two equations are applied to the scattering data contained in Hess's compilation,¹⁶ it is found that only a few measurements have been made at angles and energies of interest to our problem. Figure 2 contains a graph of all values of $\partial\sigma/\partial T'$ for T' values between 10 and 35 MeV for two extreme cases: the target neutron at rest, and the target neutron with 25 MeV of kinetic energy, since inside a real nucleus the momentum distribution of the bound neutrons is such that they all have kinetic energies between about 0 and 25 MeV. Graphs similar to that in Fig. 2 were calculated for various values of T_n , since theoretically it would then be possible to average $\partial\sigma/\partial T'$ over an assumed neutron-momentum distribution. It soon became apparent, however, that for any plausible method of averaging over ϕ and T_n , the resultant averaged $\partial\sigma/\partial T'$ is roughly

constant at about 0.1 mb/MeV in the region of interest. If we adopt this as an approximation, then,

$$\int_{\Omega_k} \frac{\partial \sigma}{\partial \Omega} d\Omega \approx 0.1(S - E_k) \quad (7)$$

and

$$\sigma(p, n) = 0.1 \sum_k a_k (S - E_k). \quad (8)$$

The coefficients a_k depend only upon the choice of oscillator frequency. We are able, therefore, to obtain an estimated (p, n) cross section for every choice of oscillator frequency, separation energy, and set of values of the hole excitation energies. The oscillator frequency is simply related to the root-mean-square radius of the least bound neutron in the target nucleus, and may be determined for each target studied by choosing values for these radii. The separation energies in the cases of Ca^{48} , V^{51} , and Ag^{109} are the neutron separation energies of the (p, n) products, but for the other products considered here, the proton separation energy is less than the neutron separation energy, and some further assumption must be made to take into account the barrier against charged-particle emission. Although a few hole excitation energies have been measured experimentally, most notably by Cohen,¹⁷ in general E_k values require a choice of model in order to be estimated. The hole excitation obtained by removing the least bound neutron from the target nucleus is zero, however; and in instances in which only the topmost two neutron states contribute substantially to the total cross section, we need to know only one additional hole energy in order to test Eq. (8). In the analysis that follows, we use the measured cross section for the (p, n) reaction in an estimation of the hole energy E_k .

In Table IV, the oscillator frequency for each target nucleus has been arbitrarily chosen such that the root-mean-square radius of the least bound neutron is equal to $1.2 \times A^{1/3}$ F. The quantity S is the sum of the Coulomb barrier for protons and the proton separation energy, or the neutron separation energy, whichever is smaller. The contribution of the least bound state has been estimated using Eq. (8), and this estimation appears in Table IV. Since we do not know the hole excitation energies appropriate to states other than the least bound, the assumption has been made that the difference between the measured cross section and the estimated contribution of the topmost neutron state is due entirely to the contribution of the next lowest state. This difference has then been used to estimate the hole excitation value of the next lowest state needed in order to have the equation yield the measured cross section when the summation is carried over just the two least bound states. The hole energy of the next lowest state that has been estimated in this manner is given in the last column of Table IV.

¹⁷ B. L. Cohen, Phys. Rev. **130**, 227 (1963).

TABLE IV. Estimated relative contributions of neutron states to the (p, n) reaction, assuming only two states are available in each case.

Target	σ (observed) (mb)	S (MeV)	K	σ_k' (mb)	$\hbar\omega$ (MeV)	E_k (MeV)
Ca^{44a}	2.0	8.1	$1f_{7/2}$	0.9	10.4	0
Ca^{48}	2.3	8.2	$1f_{7/2}$	1.8	9.8	0
			$1d_{3/2}$	0.5	7.6	2
V^{51}	2.2	9.1	$1f_{7/2}$	1.9	9.4	0
			$1d_{3/2}$	0.3	7.3	5
Cr^{52}	1.45	7.9	$1f_{7/2}$	1.6	1.6	0
			$1d_{3/2}$	0	7.0	>8
Cr^{54}	0.72	9.1	$2p_{3/2}$	0.52	9.1	0
			$1f_{7/2}$	0.20	9.1	8
Fe^{56}	0.92	7.5	$2p_{3/2}$	0.24	8.9	0
			$1f_{7/2}$	0.68	8.9	5
Ni^{64}	0.97	7.9	$1f_{5/2}$	0.75	8.1	0
			$2p_{3/2}$	0.22	8.1	6
Cu^{65}	0.74	7.9	$1f_{5/2}$	0.73	8.0	0
			$2p_{3/2}$	0.01	8.0	8
Ag^{109}	1.45	7.1	$2d_{3/2}$	0.76	6.9	0
			$1g_{7/2}$	0.69	6.9	2.6

^a See discussion.

Only one of the (p, n) reactions considered, that with Ca^{44} , diverges significantly from Eq. (8). The $1f_{7/2}$ state in Ca^{44} is predicted to contribute less than half of the observed cross section, and the $1d_{3/2}$ state cannot be made to account for all of the remainder unless the harmonic oscillator is reduced to a value that corresponds to less than 8 MeV.

IV. CONCLUSIONS

It has been suggested⁵ that high-energy (p, n) reactions might occur predominantly through the formation of the isobaric analog of the target ground state. This predominance would have the effect of favoring ($p, 2$ nucleon) cross sections at the expense of (p, n) cross sections in targets with high Coulomb displacement energies, and therefore could be detected if present. The Coulomb displacement energy of the Ag^{109} ground state has been determined by Anderson *et al.*¹⁸ to be 13 MeV, which is 5 MeV greater than the criterion used here for particle-emission stability of the Cd^{109} residual nucleus. Since the $\text{Ag}^{109}(p, n)\text{Cd}^{109}$ cross section is not unexpectedly small, this possible effect is apparently unimportant.

In this treatment of the (p, n) reaction, we have used the impulse approximation in the sense that it was assumed that all of the other nucleons in the target nucleus have no effect upon the p - n collision other than to disallow scattering of the proton into states that are already occupied. The discrete character of the states into which the proton can be scattered has not been considered.

The work of Benioff,¹ and of Porile and Tanaka,² indicates that (p, pn) formation cross sections may be predictable in terms of the total free-particle p - n

¹⁸ J. O. Anderson, C. Wong, and J. W. McClure, Phys. Rev. **129**, 2718 (1963).

collision cross section and the number and spatial distributions of target neutrons whose hole excitation energies are sufficiently small to permit the residual nucleus to be stable against particle emission. We find that the same simple model seems adequate for the estimation of the cross sections for high-energy (p,n) reactions.

Considering the crudeness of the calculation, the values of E_k in Table IV are not to be taken too seriously. The important point is that despite the crudeness

of the calculation, the E_k , which are the only free parameters in the calculation, have both reasonable values and trends with changing mass number.

ACKNOWLEDGMENTS

We should like to thank Dr. Warren Goodell, Edmund Taylor, William Hunt, and their staffs and associates for the use of the facilities of the Nevis Laboratories.

Measurement of Pair-Production Cross Section near Threshold*

TOSHIMITSU YAMAZAKI† AND JACK M. HOLLANDER

Lawrence Radiation Laboratory, University of California, Berkeley, California

(Received 17 June 1965)

A determination has been made of the total pair production cross section near threshold in germanium ($Z=32$) with use of lithium-drifted germanium gamma-ray detectors. The experimental results show a systematic trend when compared with the theoretical cross sections of Bethe and Heitler. The ratio of the experimental cross section to the Bethe-Heitler theoretical value increases as the photon energy approaches threshold; however, the increase is more rapid than expected from the calculations of Jaeger and Hulme.

I. INTRODUCTION

PAIR production is one of the fundamental processes of the interaction of photons with matter. The theoretical treatment of this process was given by Bethe and Heitler¹ (hereafter referred to as BH) in 1934. They calculated the cross section on the basis of the Born approximation in which the interaction of the created electrons with the nucleus is considered to be a small perturbation. In this approximation, the total cross section is exactly proportional to Z^2 , and decreases very rapidly as the photon energy approaches the threshold $2mc^2$. The criterion for the validity of the Born approximation is that

$$Ze^2/hv_+ \ll 1 \quad \text{and} \quad Ze^2/hv_- \ll 1,$$

where v_+ and v_- are the velocities of the created positron and negatron, respectively, and Ze is the nuclear charge. These conditions are also expressed as

$$E_+ \text{ (and } E_-) \gg 1/[1 - (\alpha Z)^2]^{1/2},$$

where E_+ and E_- are total energies of the respective particles in units of mc^2 . In other words, the necessary condition for the validity of the BH formula is that the photon energy k in units of mc^2 be

$$k \gg 2/[1 - (\alpha Z)^2]^{1/2}.$$

* This work was done under the auspices of the U. S. Atomic Energy Commission.

† On leave from the Institute for Nuclear Study, University of Tokyo, Tokyo, Japan.

¹ H. A. Bethe and W. Heitler, Proc. Roy. Soc. (London) **A146**, 83 (1934).

This means that at energies near threshold, $2mc^2$, the BH formula may not be accurate.

Later, Jaeger and Hulme² and Jaeger³ (referred to hereafter as JH) calculated the cross section as well as the energy distribution without using the Born approximation. They obtained an asymmetric energy distribution between the positron and the negatron which is caused by the repulsion of the positron from and the attraction of the negatron to the nucleus. The total cross section for Pb was found to be considerably larger below 2.6 MeV than the BH value.

Most of the experimental determinations of the total pair-production cross section, σ_{pair} , have in the past been done by means of total photon absorption measurements.⁴ The total absorption coefficient, μ_{total} , consists of three parts, i.e., the photoelectric effect, the Compton effect, and pair production. Since the cross section for the Compton scattering, σ_{Compton} , is well known from the Klein-Nishina formula and the photoeffect is negligible in the relevant energy region, σ_{pair} can be deduced from μ_{total} . There have been many experimental studies made in this way. One of them, performed by Colgate,⁵ shows (1) good agreement of the experimental cross section for any material at 2.62, 4.47, and 6.13 MeV with the theoretical value given by BH and (2) a

² J. C. Jaeger and H. R. Hulme, Proc. Roy. Soc. (London) **A153**, 443 (1936).

³ J. C. Jaeger, Nature **137**, 781 (1936); **148**, 86 (1941).

⁴ See review articles, for instance: C. M. Davisson and R. D. Evans, Rev. Mod. Phys. **24**, 79 (1952).

⁵ S. A. Colgate, Phys. Rev. **87**, 592 (1952).